3α-cluster structure of the 0^+ states in ^{12}C and the effective α-α interactions

S. I. Fedotov,[1] O. I. Kartavtsev,[2] V. I. Kochkin,[3] and A. V. Malykh[2,4]
[1]*Bogoliubov Laboratory of Theoretical Physics, Joint Institute for Nuclear Research, Dubna 141980, Russia*
[2]*Dzhelepov Laboratory of Nuclear Problems, Joint Institute for Nuclear Research, Dubna 141980, Russia*
[3]*Laboratory of Information Technologies, Joint Institute for Nuclear Research, Dubna 141980, Russia*
[4]*Physics Department, Novgorod State University, Novgorod the Great 173003, Russia*
(Received 6 April 2004; published 19 July 2004)

The 0^+ states of ^{12}C are considered within the framework of the microscopic three-α-cluster model. The main attention is paid to accurate calculation of the width of the extremely narrow near-threshold 0_2^+ state which plays a key role in stellar nucleosynthesis. It is shown that the 0_2^+-state decays by means of the sequential mechanism $^{12}\mathrm{C}\rightarrow\alpha+^{8}\mathrm{Be}\rightarrow 3\alpha$. Calculations are performed for a number of effective α-α potentials which are chosen to reproduce both energy and width of ^{8}Be. The parameters of the additional three-body potential are chosen to fix both the ground and excited state energies at the experimental values. The dependence of the width on the parameters of the effective α-α potential is studied in order to impose restrictions on the potentials.

DOI: 10.1103/PhysRevC.70.014006 PACS number(s): 21.45.+v, 21.60.Gx, 23.60.+e, 24.30.Gd

I. INTRODUCTION

The processes with few (three and more) charged particles in the initial or final state are complicated phenomena which so far have not been completely understood. The main difficulty stems from the necessity to describe the continuum wave function of three (or more) charged particles (three-body continuum). Reliable description of the continuum three-body wave function is of importance for a number of problems in nuclear physics and nuclear astrophysics. As the first example one should mention the famous nuclear reaction—formation of the ^{12}C nucleus in the triple-α low-energy collisions. This reaction is of key importance for stellar nucleosynthesis [1,2] as a unique possibility for helium burning that allows further synthesis of heavier elements. Other interesting examples of the three-body nuclear processes are double-proton radioactivity, which has been a subject of thorough experimental and theoretical investigations during the last years (more details can be found in the recent reviews [3,4]), and decay of the long-lived 1^+ state of the ^{12}C nucleus [5]. For the problems of this kind, even qualitative understanding of the reaction mechanism is crucial. In this respect, Coulomb-correlated penetration of outgoing particles through a multidimensional potential barrier has been considered in Ref. [6], thus describing qualitative features of multicluster decay of atomic nuclei.

Of key importance for description of the triple-α reaction are both the near-threshold three-body resonance (0_2^+ state of ^{12}C) predicted in Ref. [2] as the only explanation for observable abundance of elements in the universe and the low-energy α-α resonance (the ground state of ^{8}Be). Due to existence of these resonances, sufficiently fast helium burning in stars was explained by the sequential mechanism $3\alpha\rightarrow{}^{8}\mathrm{Be}+\alpha\rightarrow{}^{12}\mathrm{C}(0_2^+)\rightarrow{}^{12}\mathrm{C}+\gamma$ of the reaction. Indeed, the predicted 0_2^+ state of the ^{12}C nucleus was observed in the experiments [7,8] and was studied in the later works; in particular, the decay mechanism was a subject of investigation in Ref. [9]. The experimental studies must be supplemented by microscopic calculations to provide unambiguous determination of the decay mechanism and resonance width $\Gamma\sim 8$ eV, extremely small on the nuclear scale.

Besides the resonance triple-α reaction, it is of interest to consider in astrophysical applications, as pointed out in Ref. [10], the nonresonance reaction $3\alpha\rightarrow{}^{12}\mathrm{C}$ which takes place at low temperatures and high densities. Helium burning at such conditions is possible in accretion on white dwarfs and neutron stars. The nonresonance reaction was considered in a number of papers [11–14] based on the model assumptions; however, a consistent treatment of the three-body dynamics is lacking. In this respect, note that at ultra-low energies any approximation can lead to an error of a few orders of magnitude in the calculated reaction rate.

Besides astrophysical applications, studies of the three-α scattering provide important information about the effective α-α interaction which is of interest for the α-cluster calculations. As the α-particle is the most tightly bound nucleus, many low-energy nuclear properties can be successfully calculated within the framework of the α-cluster model [15–20]. Generally, the three-body calculations allow one to reduce the uncertainty in the two-body potential which can be hardly determined only from the two-body data. One of the principal opportunities for unambiguous determination of the α-α effective potential is to set the calculated width of the 0_2^+ three-body resonance to its experimental value. In addition, one should mention that recently the near-threshold α-cluster states have attracted a special attention in connection with α-particle condensation in low-density nuclear matter [21,22].

In this paper, properties of the 0^+ states of ^{12}C are considered using the 3α-cluster model with the main emphasis on the calculation of the width of the near-threshold 0_2^+ state. Calculations are performed for a number of effective α-α potentials which are chosen to reproduce with a good accuracy both the energy and the width of the α-α resonance (ground state of ^{8}Be). Furthermore, due to the strong exponential dependence of the resonance width on the resonance

 ©2004 The American Physical Society

energy, calculation of the width makes sense only if the resonance position is fixed. For the 3-α resonance under consideration, this requirement is satisfied by adjusting the parameters of the additional three-body potential which must be introduced to describe the effect of α-particle distortions near the triple-collision point. More precisely, the three-body potential is chosen to fix both the ground and excited state energies at the experimental values. Following Ref. [23], the method of calculation is based on the expansion of the total wave function in terms of the eigenfunctions on a hypersphere (at a fixed hyper-radius), which allows solving both the eigenvalue problem for the ground state and the scattering problem for the excited resonance state. The eigenfunctions on a hypersphere are calculated by using the variational method with a flexible set of trial functions which describe properly the three-body wave function both at large and small interparticle distances.

The present three-body calculation of the near-threshold resonance is the first necessary step in the unified treatment of the low-energy triple-α reaction. Both the method and the numerical procedure can be used to calculate the reaction rate at lower energies where the resonance mechanism turns to the nonresonance one.

II. METHOD

The present paper is aimed at microscopic description of the low-energy scattering of three α-particles whose features are to a great extent determined by the two- and three-body resonances. In this respect, the principal problem is reliable calculation of characteristics of the extremely narrow near-threshold resonance (0_2^+-state of ^{12}C). The α-cluster model that is used allows for taking account of the most important features of the wave function, i.e., the three-α-cluster and two-cluster $\alpha+^8$Be components. All the effects connected with both the internal structure of α-particles and the identity of nucleons are incorporated in the effective α-α potential. Besides, the additional three-body potential of a simple Gaussian form as in papers [16,17] is introduced to describe the effects beyond the three-cluster approximation. Thus, the model allows description of both the ground and the excited 0^+ states of ^{12}C. Considering the challenging problem of reliable calculation of the 0_2^+ resonance width, the effective two-body potential should satisfy the restriction that the position and width of ^{8}Be are fixed at the experimental values. In a similar way, the three-body potential will be chosen to obtain experimental energies for both ground and excited states of ^{12}C.

For the low-energy scattering in question, one should consider only the 0^+ states (the total angular momentum $L=0$). The units $\hbar=m=e=1$ are used throughout the paper unless other is specified. The Schrödinger equation for three α-particles reads

$$\left(-\Delta_{\mathbf{x}_i}-\Delta_{\mathbf{y}_i}+\sum_{j=1}^{3}V(x_j)+V_3(\rho)-E\right)\Psi=0, \tag{1}$$

where the scaled Jacobi coordinates are $\mathbf{x}_i=\mathbf{r}_j-\mathbf{r}_k$, $\mathbf{y}_i=(2\mathbf{r}_i-\mathbf{r}_j-\mathbf{r}_k)/\sqrt{3}$ and $\mathbf{r}_i$ is the position vector of the ith particle. In the following it is convenient to use the hyperspherical coordinates $0\leqslant\rho<\infty$, $0\leqslant\alpha_i\leqslant\pi$, and $0\leqslant\theta_i\leqslant\pi$ defined as

$$x_i=\rho\cos\frac{\alpha_i}{2},\quad y_i=\rho\sin\frac{\alpha_i}{2},\quad \cos\theta_i=\frac{(\mathbf{x}_i\mathbf{y}_i)}{x_iy_i}. \tag{2}$$

In the Schrödinger equation (1) the effective two-body potential $V(x)$ is a sum of the short-range and Coulomb interactions

$$V(x)=V_s(x)+\frac{4}{x}, \tag{3}$$

where the short-range α-α potential

$$V_s(x)=V_re^{-\mu_r^2x^2}-V_ae^{-\mu_a^2x^2} \tag{4}$$

is obtained by modification of the Ali-Bodmer potentials [24]. The three-body potential

$$V_3(\rho)=V_0e^{-(\rho/b)^2} \tag{5}$$

is chosen as the same function of the hyper-radius ρ as used in Refs. [16,17].

A. Eigenfunctions on the hypersphere

In terms of the hyperspherical variables the Schrödinger equation (1) for $L=0$ reads

$$\left[-\frac{1}{\rho^5}\frac{\partial}{\partial\rho}\left(\rho^5\frac{\partial}{\partial\rho}\right)-\frac{4}{\rho^2}\Delta^*+\sum_{j=1}^{3}V\left(\rho\cos\frac{\alpha_j}{2}\right)+V_3(\rho)-E\right]\Psi=0, \tag{6}$$

where

$$\Delta^*=\frac{1}{\sin^2\alpha_i}\left[\frac{\partial}{\partial\alpha_i}\left(\sin^2\alpha_i\frac{\partial}{\partial\alpha_i}\right)+\frac{1}{\sin\theta_i}\frac{\partial}{\partial\theta_i}\left(\sin\theta_i\frac{\partial}{\partial\theta_i}\right)\right] \tag{7}$$

is the grand angular momentum operator up to a constant factor. In order to solve both the eigenvalue and scattering problems for Eq. (6) the total wave function is expanded in a series

$$\Psi=\rho^{-5/2}\sum_n f_n(\rho)\Phi_n(\alpha,\theta,\rho) \tag{8}$$

on a discrete set of eigenfunctions Φ_n of the following equation on the hypersphere:

$$\left[\Delta^*-\frac{\rho^2}{4}\sum_{j=1}^{3}V\left(\rho\cos\frac{\alpha_j}{2}\right)+\lambda_n(\rho)\right]\Phi_n(\alpha,\theta,\rho)=0, \tag{9}$$

as proposed in Ref. [23]. At each ρ the index $n=1,2,3,\ldots$ enumerates the eigenvalues λ_n in ascending order and the eigenfunctions $\Phi_n(\alpha,\theta,\rho)$ are normalized by the conditions $\langle\Phi_n|\Phi_m\rangle=\delta_{nm}$ where the notation $\langle\cdot|\cdot\rangle$ means the integration over the invariant volume on the hypersphere $d\Omega=\sin^2\alpha_i d\alpha_i d\cos\theta_i$. Due to identity of α-particles both the total wave function Ψ and the eigenfunctions $\Phi_n(\alpha,\theta,\rho)$ are symmetric under any permutation of particles i, j, and k.

Given the expansion (8) of the total wave function, the Schrödinger equation (6) is reduced to the system of hyperradial equations (HREs),

$$\left[\frac{\partial^2}{\partial\rho^2}-\frac{1}{\rho^2}\left(4\lambda_n(\rho)+\frac{15}{4}\right)+V_3(\rho)+E\right]f_n(\rho) + \sum_m\left(Q_{nm}(\rho)\frac{\partial}{\partial\rho}+\frac{\partial}{\partial\rho}Q_{nm}(\rho)-P_{nm}(\rho)\right)f_m(\rho)=0, \tag{10}$$

where

$$Q_{mn}(\rho)=\left\langle\Phi_m\left|\frac{\partial\Phi_n}{\partial\rho}\right.\right\rangle, \tag{11}$$

$$P_{mn}(\rho)=\left\langle\frac{\partial\Phi_m}{\partial\rho}\left|\frac{\partial\Phi_n}{\partial\rho}\right.\right\rangle. \tag{12}$$

The coefficients $\lambda_n(\rho)$, $Q_{nm}(\rho)$, and $P_{nm}(\rho)$ of HRE (10) are calculated using the variational method for solution of the eigenvalue problem (9). The variational basis consists of N trial functions χ_i with the same symmetry under permutations of particles as the eigenfunctions $\Phi_n(\alpha,\theta,\rho)$. In view of an essentially different structure of the eigenfunctions $\Phi_n(\alpha,\theta,\rho)$ at different values of ρ, it is necessary to use a flexible basis of trial functions which allows one to describe the two- and three-cluster structure of the wave function in the asymptotic region.

First of all, the basis contains a set of the symmetric hyperspherical harmonics (SHH) H_{nm} which are the eigenfunctions of the operator Δ^*, i.e.,

$$[\Delta^*+K(K+2)]H_{nm}=0, \tag{13}$$

where $K=2n+3m$, the non-negative numbers n and m enumerate SHH, and $2K$ is the order of SHH. For explicit construction of SHH it is convenient to use another set of the hyperspherical variables $0\leqslant\xi\leqslant\pi/2$, $-\pi\leqslant\varphi_i\leqslant\pi$ [25,26], defined by

$$\begin{aligned}\sin\xi&=\sin\alpha_i\sin\theta_i,\\ \cos\xi\cos\varphi_i&=\cos\alpha_i,\\ \cos\xi\sin\varphi_i&=\sin\alpha_i\cos\theta_i.\end{aligned} \tag{14}$$

In these variables

$$\begin{aligned}H_{nm}(\xi,\varphi)&\sim\cos^{3m}\xi P_n^{(0,3m)}(\cos2\xi)T_{3m}(\cos\varphi)\\ &\sim d^{n+(3/2)m}_{(3/2)m,(3/2)m}(2\xi)\cos3m\varphi,\end{aligned} \tag{15}$$

where $P_n^{(\alpha,\beta)}(x)$ and $T_n(x)$ are the Jacobi and Chebyshev polynomials and $d^j_{mk}(\beta)$ is the Wigner function. The variable ξ is invariant under permutations of particles and, therefore, is independent of the index i enumerating the Jacobi variables. On the other hand, φ_i changes to $\varphi_i\pm2\pi/3$ under the cyclic permutations as $|\varphi_i-\varphi_j|=2\pi/3$ and $\varphi_i\to-\varphi_i$ under the permutation of particles j and k. As follows from Eq. (15) and the above properties of the variables ξ and φ_i, SHH are completely symmetric under any permutation.

In the numerical calculations, the basis of trial functions contains a set of all SHH $\chi_i(\alpha,\theta)=H_{n_im_i}(\xi,\varphi)$ with those indices n_i and m_i for which K does not exceed the maximum value $K_{\max}$, i.e., $K_i=2n_i+3m_i\leqslant K_{\max}$. One can count that the total number of such SHH for which $2n_i+3m_i\leqslant K$ equals $K(K+6)/12+1$ for K being a multiple of 6 and $([K/6]+1)(K-3[K/6])$ otherwise. Here $[x]$ stands for the entire part of x. Usage of SHH in the basis of trial functions provides an excellent description of the eigenfunctions at small ρ, where the kinetic energy term dominates, and quite a good description at intermediate ρ, where the cluster effects still do not dominate. However, the two-cluster component of the wave function corresponding to the configuration $\alpha+{}^8$Be can be hardly described by a set of SHH due to rather slow convergence that hinders the calculation at sufficiently large ρ.

In order to describe the two-cluster configuration, the basis of trial functions should also include the ρ-dependent symmetric combinations

$$\chi_i(\alpha,\theta)=\sum_{j=1}^{3}\phi_i\left(\rho\cos\frac{\alpha_j}{2}\right) \tag{16}$$

of the two-body functions $\phi_i(x)$ which are chosen to describe the wave function of the two-body α-α resonance. More precisely, a set of $\phi_i(x)$ includes a few Gaussian functions

$$\phi_i(x)=\exp(-\beta_i x^2) \tag{17}$$

which allows the two-body wave function to be described, with properly chosen parameters β_i, within the range of the nuclear potential $V_s(r)$. In addition, the function

$$\phi(x)=x^{1/4}\exp(-4\sqrt{x}(1+ax)) \tag{18}$$

is used to describe the two-body wave function in the under-barrier region. This latter function is of the asymptotic form of the Coulomb wave function which is optionally cut off by the parameter a at large distances.

Although the eigenvalues $\lambda_n(\rho)$ are directly determined in the variational calculation, the coupling terms $Q_{nm}(\rho)$ and $P_{nm}(\rho)$ can hardly be determined by means of definitions (11) and (12), which is hindered due to the necessity of calculating the derivatives $\partial\Phi_n/\partial\rho$. For this reason, $Q_{nm}(\rho)$ are calculated by using the exact expression

$$Q_{mn}(\rho)=\frac{3}{4}(\lambda_n-\lambda_m)^{-1}\left\langle\Phi_m\left|\frac{q}{\cos\alpha}+2\rho V_s\left(\rho\cos\frac{\alpha}{2}\right)+\rho^2\frac{\partial V_s(\rho\cos\alpha/2)}{\partial\rho}\right|\Phi_n\right\rangle, \tag{19}$$

which is derived by differentiating the eigenvalue equation (7) with respect to ρ and projecting the result on the function Φ_m. Furthermore, $P_{nm}(\rho)$ are calculated by using the exact sum rule $P=-Q^2$ for the matrices P and Q, which leads to the approximation

$$P_{mn}(\rho)=\sum_{l=1}^{N}Q_{ml}(\rho)Q_{nl}(\rho) \tag{20}$$

on the limited basis of N trial functions.

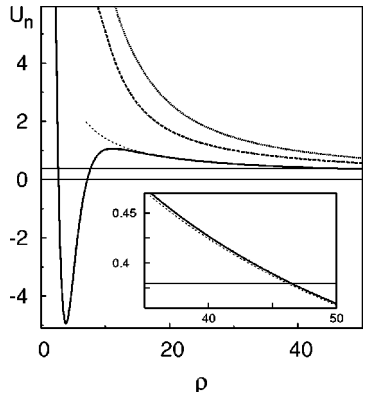

FIG. 1. Three lowest effective potentials $U_n(\rho)$. Shown are also the asymptotic two-cluster dependence $U_1(\rho) \approx E_{2\alpha} + \tilde{q}/\rho$ (thin dashed line) and the energy of the 0_2^+ state $E = 0.3795$ MeV (thin horizontal line).

B. Boundary conditions and characteristics of ^{12}C states

Properties of the ground 0_1^+ state and the excited 0_2^+ resonance are determined by solving the eigenvalue problem (at $E<0$) and scattering problem (at $E>0$) for HRE (10), respectively. Denote the hyper-radial functions as $f_n^{(1)}(\rho)$ for the ground state and $f_n^{(E)}(\rho)$ for the scattering problem at energy E. According to (8), all these functions satisfy the zero boundary conditions at $\rho = 0$. The square integrable solution of HRE (10) satisfying the condition

$$\sum_n \int_0^\infty |f_n^{(1)}(\rho)|^2 d\rho = 1 \tag{21}$$

unambiguously determines the energy $E_{\text{g.s.}}$ and the wave function of the ground 0_1^+ state.

The position E_r and width Γ of the near-threshold 0_2^+ resonance are calculated by solving HRE (10) with the asymptotic boundary conditions corresponding to the ingoing wave in the first channel, i.e., $f_1^{(E)}(\rho)$ is a sum of the ingoing and outgoing waves in the effective potential $U_1(\rho) = (1/\rho^2)\left[4\lambda_1(\rho) + \frac{15}{4}\right] + P_{11}(\rho)$. More precisely, the asymptotic boundary conditions are imposed near the turning point ρ_t of the first-channel effective potential defined by the condition $U_1(\rho_t) = E$. As expected, calculations reveal (see also Fig. 1) that at $\rho \sim \rho_t$ the effective potential $U_1(\rho)$ is to a good approximation expressed as

$$U_1(\rho) \approx E_{2\alpha} + \frac{\tilde{q}}{\rho}, \tag{22}$$

where $E_{2\alpha}$ is the energy of the two-body resonance (the ground state of ^{8}Be) and the Coulomb parameter $\tilde{q} = 16/\sqrt{3}$. In fact, r.h.s. of Eq. (22) is the energy of the two-cluster system $\alpha + {}^8$Be at a large fixed hyper-radius ρ. For the scattering at energy above the two-body resonance ($E > E_{2\alpha}$), in view of expression (22), the first channel hyper-radial function can be written as

$$f_1^{(E)}(\rho) \sim F_0(\eta, k\rho) + \tan\delta_E G_0(\eta, k\rho) \tag{23}$$

in the range of hyper-radius values $\rho \sim \rho_t$. Here the wave number in the first channel is $k = \sqrt{E - E_{2\alpha}}$, $F_0(\eta, k\rho)$ and $G_0(\eta, k\rho)$ are the Coulomb functions with the parameter $\eta = 8/(\sqrt{3}k)$, and δ_E is the scattering phase shift. Due to strong repulsive potentials $U_n(\rho)$ for $n \geqslant 2$ the outgoing waves in the upper channels are negligible at small energies $E \leqslant 1$ MeV. This allows the zero boundary conditions

$$f_n^{(E)}(\rho) = 0 \tag{24}$$

to be imposed at some value of the hyper-radius $\rho > \rho_t$ for all $n \geqslant 2$. The resonance position E_r and width Γ as well as the nonresonant phase shift δ_{bg} are defined by fitting the calculated near-resonance phase shift δ_E to the Wigner dependence on energy

$$\cot(\delta_E - \delta_{bg}) = \frac{2}{\Gamma}(E - E_r). \tag{25}$$

In the following description of the 0_2^+ state it is suitable to treat the ultra-narrow resonance as a true bound state with the wave function $f_n^{(2)}(\rho) \sim f_n^{(E_r)}(\rho)$ corresponding to the scattering solution at the resonance energy E_r and normalized on the finite interval $0 \leqslant \rho \leqslant \rho_t$ by the condition

$$\sum_n \int_0^{\rho_t} |f_n^{(2)}(\rho)|^2 d\rho = 1. \tag{26}$$

It is of interest to determine also the root-mean-square (rms) radii

$$R^{(i)} = \frac{1}{N_t}\sum_k^{N_t} \langle \Psi^{(i)} | (\mathbf{r}_k - \mathbf{R}_{cm})^2 | \Psi^{(i)} \rangle \tag{27}$$

of the ground ($i=1$) and excited ($i=2$) states and the monopole transition matrix element

$$M_{12} = \sum_k^{N_p} \langle \Psi^{(1)} | (\mathbf{r}_k - \mathbf{R}_{cm})^2 | \Psi^{(2)} \rangle. \tag{28}$$

A sum is taken over N_t nucleons in (27) and over N_p protons in (28) and $\mathbf{R}_{\text{c.m.}}$ is the center-of-mass position vector. Following the definitions (27) and (28), in the three-α-particle model one obtains the expressions

$$R^{(i)} = \sqrt{R_\alpha^2 + \tfrac{1}{6}\overline{\rho_i^2}}, \tag{29}$$

$$M_{12} = \sum_n \int_0^{\rho_t} f_n^{(2)}(\rho) f_n^{(1)}(\rho) \rho^2 d\rho, \tag{30}$$

where $R_\alpha = 1.47$ fm is the rms radius of the α-particle and the rms value of the hyper-radius $\overline{\rho_i^2}$ for the ith state in the three-body model is defined by

$$\overline{\rho_i^2} = \sum_n \int_0^\infty |f_n^{(i)}(\rho)|^2 \rho^2 d\rho. \tag{31}$$

TABLE I. Parameters of the short-range α-α potential V_s (4) and the corresponding widths γ of the α-α resonance (the ground state of ^{8}Be).

	V_r (MeV)	μ_r (fm^{-1})	V_a (MeV)	μ_a (fm^{-1})	γ (eV)
1	82.563	1/1.53	26.1	1/2.85	6.80
2	279.206	1/1.53	40	1/2.85	8.53
3	20.012	1/1.53	16.5	1/2.85	5.11
4	197.680	0.7	80	0.475	5.10

III. NUMERICAL RESULTS

Calculations have been performed with four $\alpha-\alpha$ potentials which are obtained by modification of potentials (a) and (d) from Ref. [24]. The parameters of the potentials have been chosen to reproduce the experimental value of the $\alpha-\alpha$ resonance (^{8}Be) energy $E_{2\alpha}=91.89$ keV whereas resonance widths have been allowed to vary within the experimental uncertainty ±1.7 eV. The parameters of the potentials and the corresponding $\alpha-\alpha$ resonance widths γ are presented in Table I. Only the strengths V_r and V_a of the repulsive and attractive parts are varied for potentials 1–3, while the parameters μ_r and μ_a are modified for "harder" potential 4. This choice of the potentials makes it possible to study the dependence of the three-body characteristics on the shape of the two-body potential.

The energies of the ground and excited states $E_{\text{g.s.}}$ and E_r, width of the excited state Γ, rms radii $R^{(i)}$, and monopole transition matrix element M_{12} for the three-α system are calculated, as discussed in the preceding section, by numerical solution of HRE (10) with boundary conditions (23) and (24). For the eigenvalue problem, numerical integration in the interval $0<\rho\leqslant 25$ fm provides the relative accuracy not worse than 10^{-6} for the calculated binding energy. For the scattering problem, numerical integration is carried out in the interval $0\leqslant\rho\leqslant\rho_{max}$ so that $\rho_{max}\sim 50$ fm is chosen beyond the turning point $\rho_t\approx 45$ fm for the first-channel effective potential $U_1(\rho)$. Choice of the parameters of the numerical integration does not affect the final results, i.e., the accuracy of the calculated $E_{\text{g.s.}}$, E_r, Γ, $R^{(i)}$, M_{12} depends merely on the accuracy of the numerical calculation for $\lambda_n(\rho)$, $P_{mn}(\rho)$, and $Q_{mn}(\rho)$. In every calculation, i.e., for each two-body potential and each number of HRE N_1, the parameters V_0 and b of the three-body potential $V_3(\rho)$ are chosen to fix the calculated E_r and $E_{\text{g.s.}}$ at the experimental values $E_r=0.3795$ MeV and $E_{\text{g.s.}}=-7.2747$ MeV.

For the calculation of the HRE coefficients $\lambda_n(\rho)$, $P_{mn}(\rho)$, and $Q_{mn}(\rho)$ by the variational method, two different sets of trial functions were used in the interval $\rho\leqslant 20$ fm and in the asymptotic region $\rho>20$ fm. At $\rho\leqslant 20$ fm the basis of trial functions contains 147 SHH, which corresponds to $K_{max}=39$. Recall that convergence with a number of SHH becomes very slow with increasing hyper-radius. For this reason, at $\rho>20$ fm the basis of trial functions contains 108 SHH ($K_{max}=33$) and four trial functions which describe the cluster configuration $\alpha+^8$Be, namely, three functions of the form (17) and one function of the form (18). The ρ-independent parameters β_i in functions (17) were determined by minimizing the first eigenvalue $\lambda_1(\rho)$. The calculated $\lambda_n(\rho)$, $P_{mn}(\rho)$, and $Q_{mn}(\rho)$ practically do not depend on the basis of trial functions near $\rho=20$ fm, which allows matching the results of calculation with two different basises. The three lowest effective potentials $U_n(\rho)=1/\rho^2\left[4\lambda_n(\rho)+\frac{15}{4}\right]+P_{nn}(\rho)$ $(n=1-3)$ for two-body potential 3 are depicted for illustration in Fig. 1.

The detailed information on the three-body system can be obtained by considering the eigenfunctions on a hypersphere $\Phi_n(\xi,\varphi,\rho)$. Due to symmetry, $\Phi_n(\xi,\varphi,\rho)$ are periodic functions of the variable φ with the period $2\pi/3$. As the main contribution to the total wave function comes from the first term $(n=1)$ of expansion (8), the first eigenfunction $\Phi_1(\xi,\varphi,\rho)$ practically determines the structure of the system. For illustration, three-dimensional plots of the first eigenfunction $\Phi_1(\xi,\varphi,\rho)$ (for two-body potential 3) are shown in Fig. 2 at three values of the hyper-radius $\rho=5$ fm, $\rho=15$ fm, and $\rho=45$ fm that correspond, as seen in Fig. 1, to the minimum, the maximum, and the turning point of $U_1(\rho)$ at $E=0.3795$ MeV. For all values of the hyper-radius, $\Phi_1(\xi,\varphi,\rho)$ is small at the zero distance between a pair of α-particles, i.e., at the point $\xi=0$, $\varphi=\pi/3$ at the hypersphere, because of the strong repulsive term in the short-range potential V_s. At sufficiently large ρ (near the turning point), $\Phi_1(\xi,\varphi,\rho)$ exhibits a specific structure concentrated in the region where the two-body potential is attractive, i.e., around the point $\xi=0$, $\varphi=\pi/3$. This structure corresponds to the two-cluster configuration $\alpha+^8$Be. For smaller values of ρ (as seen in Fig. 2 at $\rho=15$ fm) the two-cluster structure widens; besides, visible values of $\Phi_1(\xi,\varphi,\rho)$ appear both at the point $\xi=\pi/2$, which corresponds to the configuration of the equilateral triangle, and near the point $\xi=0$, $\varphi=0$ (or $\xi=0$, $\varphi=2\pi/3$), which corresponds to the linear configuration. Next, at small ρ near the minimum of $U_1(\rho)$, the most important is the triangle configuration with a noticeable weight of the linear configuration and without any trace of the two-cluster structure.

The accuracy of the calculation is estimated by observing the convergence with increasing number of SHH. As a result, the accuracy of the most significant effective potential $U_1(\rho)$ turns out to be not worse than 1 eV in the entire interval $0<\rho\leqslant 20$ fm and is much better for smaller ρ. In a similar way, the relative accuracy of $P_{mn}(\rho)$ and $Q_{mn}(\rho)$ is better than 10^{-5} in the same interval $0<\rho\leqslant 20$ fm. As the hyper-radius increases beyond $\rho=20$ fm, the accuracy of the calculation decreases due to a more complicated structure of the eigenfunctions $\Phi_1(\xi,\varphi,\rho)$. Nevertheless, as shown in Fig. 1, the effective potential $U_1(\rho)$ is in good agreement with the asymptotic dependence (22) in the interval $40\leqslant\rho\leqslant 60$, thus pointing to the sufficiently high accuracy. In particular, for all the potentials used, a fit of $U_1(\rho)$ to Eq. (22) gives the values of the Coulomb parameter $\tilde{q}$ which differ from the expected value $\tilde{q}=13.3$ MeV·fm by less than 0.14 MeV·fm. The fitted values of $E_{2\alpha}$ differ from the experimental energy of ^{8}Be by less than 0.004 MeV for potentials $1-3$ and by about 0.009 MeV for potential 4.

Note that representation (22) of the effective potential $U_1(\rho)$ in terms of the energy of the two-cluster system α

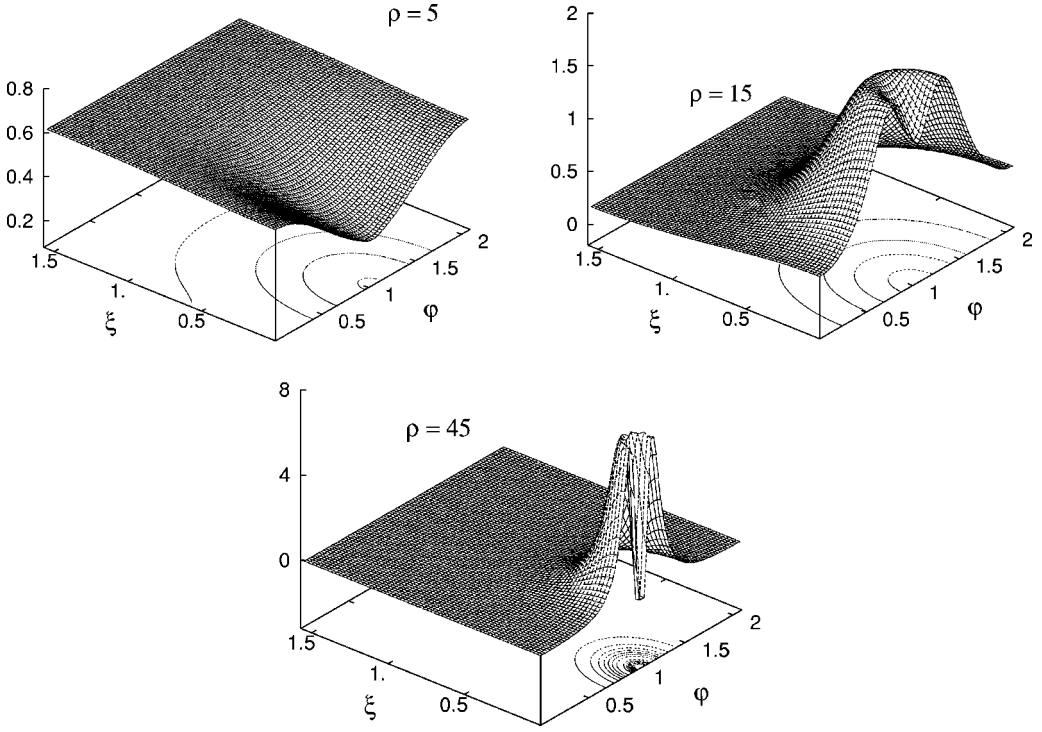

FIG. 2. The first eigenfunction $\Phi_1(\xi,\varphi,\rho)$ at different ρ.

$+{}^8$Be confirms the sequential mechanism of 0_2^+ state decay with formation of $\alpha+{}^8$Be at the first step. Also, this conclusion follows from the genuine two-cluster form of the first-channel eigenfunction $\Phi_1(\xi,\phi,\rho)$ at $\rho\approx\rho_t$. As shown in Fig. 2 at $\rho=45$ fm, $\Phi_1(\xi,\phi,\rho)$ practically coincides with the symmetric combination of the ^{8}Be wave functions. Thus the total width is determined by the two-cluster decay width.

The calculated Γ, $R^{(i)}$ $(i=1,2)$, M_{12}, and the parameters of the three-body potential V_0 and b are presented in Table II for four two-body potentials and different numbers of HRE N_1. These results are compared with the experimental values and calculations [16,17] (the factor $\sqrt{2}$ in the last column appears due to different definitions of ρ in these papers). As shown in Table II, the convergence in a number of HREs is sufficiently fast and solution of three HREs ($N_1=3$) allows the resonance width to be determined with the accuracy about 1 eV. The final accuracy of Γ depends mainly on the accuracy of the variational calculation and can be estimated as a few eV. The values of the parameter b presented in Table II are quite reasonable since they are in agreement with the value $\rho=2\sqrt{2}R_\alpha\approx 4.16$ fm, which corresponds to triple collision of three hard spheres with radii R_α.

IV. DISCUSSION AND CONCLUSION

The main result of the present calculation is accurate determination of an extremely narrow width Γ of the three-body resonance (the excited 0_2^+ state of ^{12}C). As shown in Tables I and II, the width Γ of the three-body resonance depends on the underlying two-body α-α potential and essentially increases with increasing width γ of the two-body α-α resonance. In fact, variation of γ within the limits of the experimental uncertainty gives rise to a change of Γ by a factor 2.6; therefore, the precise value of γ is necessary for determination of Γ. Note that for all the potentials considered, the calculated Γ overestimate the experimental value $\Gamma_{exp}=8.5\pm1$ eV by a factor 1.2–3.1. However, the difference

TABLE II. Characteristics of the 0^+ states of three α-particles for four α-α potentials calculated with N_1 HRE. The width of the excited state Γ, the rms radii $R^{(1)}$ and $R^{(2)}$, the monopole transition matrix element M_{12}, and the parameters V_0 and b of the three-body potential are given. The results of the calculations [16,17] and the experimental values are given in the last rows.

	N_1	Γ (eV)	$R^{(1)}$ (fm)	$R^{(2)}$ (fm)	M_{12} (fm^2)	V_0 (MeV)	b (fm)
	1	25	2.56	4.1	9.52	−21.998	4.8993
1	2	20	2.55	4.1	9.08	−23.993	4.6608
	3	19	2.55	4.0	9.03	−24.048	4.6530
	1	37	2.82	4.4	10.3	−29.291	5.1213
2	2	27	2.77	4.2	9.00	−39.124	4.5223
	3	26	2.77	4.2	8.85	−39.947	4.4858
	1	13	2.25	3.6	8.23	−15.812	4.4506
3	2	11	2.24	3.6	8.15	−16.059	4.3964
	3	10	2.24	3.5	8.14	−16.066	4.3942
	1	21	2.51	4.1	8.74	−14.548	5.7248
4	2	16	2.49	4.0	8.36	−15.129	5.4595
	3	15	2.49	4.0	8.21	−15.285	5.4118
[16]		20	2.36		6.54	−96.8	$3.9/\sqrt{2}$
[17]		1300	2.47		8.36	−23.32	$3.795\cdot\sqrt{2}$
Exp.		8.5 ± 1.0	2.47		5.7		

of the calculated width for potential 3 and the experimental value is of order of the theoretical and experimental uncertainties. In addition, comparing the results for potentials 3 and 4, one may conclude that width Γ of the three-body resonance depends on the potential shape (on the parameters μ_r and μ_a). It should be emphasized that dependence of Γ on the parameters of the α-α interaction is rather complicated due to addition of the three-body potential $V_3(\rho)$ which is chosen to fix $E_{\text{g.s.}}$ and E_r at the experimental values. Nevertheless, the effect of $V_3(\rho)$ is not overwhelming since Γ is mainly determined by penetrability of the potential barrier and all the three-body potentials used in the present calculation are rapidly decreasing with increasing ρ in the barrier region 10 fm$<\rho<$45 fm.

Similar dependence on γ is revealed for the ground-state rms radius $R^{(1)}$. It is interesting that the calculated $R^{(1)}$ =2.55 fm is close to the experimental value $R^{(1)}_{exp}$=2.47 fm for potential 1, for which the two-body width γ coincides with the most probable experimental value γ_{exp}=6.8 eV. Similar to Γ, the calculated $R^{(1)}$ essentially depends on the parameters μ_r and μ_a. Both the rms radius $R^{(2)}$ of the exited states and the monopole transition matrix element M_{12} are weakly dependent on the parameters of the two-body potential. For all the potentials, the calculated values of M_{12} significantly overestimate the experimental value 5.7 fm^2 that clearly deserves further investigation.

Comparison with the previous microscopic calculation [16] shows that the accuracy of the present calculation is much better than in Ref. [16] whereas the methods of calculation are similar to each other. Note that the α-α potential in Ref. [17] was chosen to fix the rms radius of the ground state at the experimental value $R^{(1)}_{exp}$=2.47 fm. With this potential, the energy of the three-body resonance is misplaced by 0.47 MeV. This is essentially above the experimental values and leads to an unreliably large resonance width.

The above discussion allows the conclusion that calculation of three-body observables can be used to impose restriction on the effective two-body α-α potential. In the future one should look for a possibility of reproducing the experimental values by a refined choice of potentials, in particular, by using more complicated three-body potentials.

In conclusion, the three-α-cluster model is used to calculate the characteristics of the 0^+ states in the ^{12}C nucleus. In particular, the width of the extremely narrow threshold 0^+_2 state is calculated with a good accuracy. The dependence of the width on the parameters of the α-α potential is studied. It is proposed to use the calculation of the width for selection of α-α potentials. It is directly shown in the three-body calculation that the 0^+_2 state decays by means of the sequential mechanism ($^{12}\text{C}\rightarrow\alpha+^8\text{Be}\rightarrow 3\alpha$). This conclusion is in agreement with the experiment [9] in which the rate of the direct decay $^{12}\text{C}\rightarrow 3\alpha$ is estimated to be less than 1% of the total rate. The calculation of the near-threshold 3α-resonance can be considered as a part of the general study of both resonant and nonresonant reaction $3\alpha\rightarrow{}^{12}$C at low energy. The present approach is promising for calculation of the triple-α reaction rate at low energy below the three-body resonance. This provides an opportunity for unified treatment of the crossover from the resonant to the nonresonant mechanism of the reaction.

[1] E. E. Salpeter, Astrophys. J. **115**, 326 (1952).
[2] F. Hoyle, Astrophys. J., Suppl. **1**, 121 (1954).
[3] L. V. Grigorenko, R. C. Johnson, I. G. Mukha, I. J. Thompson, and M. V. Zhukov, Phys. Rev. C **64**, 054002 (2001).
[4] L. V. Grigorenko and M. V. Zhukov, Phys. Rev. C **68**, 054005 (2003).
[5] H. O. U. Fynbo *et al.*, Phys. Rev. Lett. **91**, 082502 (2003).
[6] O. I. Kartavtsev, Few-Body Syst. (to be published).
[7] D. N. F. Dunbar, R. E. Pixley, W. A. Wenzel, and W. Whaling, Phys. Rev. **92**, 649 (1953).
[8] C. W. Cook, W. A. Fowler, C. C. Lauritsen, and T. Lauritsen, Phys. Rev. **107**, 508 (1957).
[9] M. Freer *et al.*, Phys. Rev. C **49**, R1751 (1994).
[10] A. G. W. Cameron, Astrophys. J. **130**, 916 (1959).
[11] K. Nomoto, F.-K. Thielemann, and S. Miyaji, Astron. Astrophys. **149**, 239 (1985).
[12] K. Langanke, M. Wiescher, and F. K. Thielemann, Z. Phys. A **324**, 147 (1986).
[13] I. Fushiki and D. Q. Lamb, Astrophys. J. **317**, 368 (1987).
[14] S. Schramm, Astrophys. J. **397**, 579 (1992).
[15] P. Pichler, H. Oberhummer, A. Csótó, and S. A. Moszkowski, Nucl. Phys. **A618**, 55 (1997).
[16] D. V. Fedorov and A. S. Jensen, Phys. Lett. B **389**, 631 (1996).
[17] N. N. Filikhin, Yad. Fiz. **63**, 1612 (2000).
[18] N. N. Filikhin and S. L. Yakovlev, Yad. Fiz. **63**, 409 (2000).
[19] P. Descouvemont and D. Baye, Phys. Rev. C **36**, 54 (1987).
[20] Y. Kanada-En'yo, Phys. Rev. Lett. **81**, 5291 (1998).
[21] A. Tohsaki, H. Horiuchi, P. Schuck, and G. Röpke, Phys. Rev. Lett. **87**, 192501 (2001).
[22] T. Yamada and P. Schuck, Phys. Rev. C **69**, 024309 (2004).
[23] J. H. Macek, J. Phys. B **1**, 831 (1968).
[24] S. Ali and A. R. Bodmer, Nucl. Phys. **80**, 99 (1966).
[25] F. T. Smith, J. Math. Phys. **3**, 375 (1962).
[26] A. Dragt, J. Math. Phys. **6**, 533 (1965).